Host transcription factor Speckled 110 kDa (Sp110), a nuclear body protein, is hijacked by hepatitis B virus protein X for viral persistence

Received for publication, May 16, 2017, and in revised form, October 13, 2017 Published, Papers in Press, October 18, 2017, DOI 10.1074/jbc.M117.796839

Isha Sengupta[‡], **Dipanwita Das**[§], **Shivaram Prasad Singh**[¶], **Runu Chakravarty**[§], **and Chandrima Das**[‡1]

From the [‡]*Biophysics and Structural Genomics Division, Saha Institute of Nuclear Physics, Kolkata-700064, the* [§]*Indian Council of Medical Research (ICMR) Virus Unit, Kolkata, Infectious Diseases and Beliaghata General Hospital Campus, Kolkata 700010, and the* [¶]*Kalinga Gastroenterology Foundation, Beam Diagnostics Premises, Cuttack-753001, India*

Edited by Charles E. Samuel

Promyelocytic leukemia nuclear bodies (PML-NB) are subnuclear organelles that are the hub of numerous proteins. DNA/RNA viruses often hijack the cellular factors resident in PML-NBs to promote their proliferation in host cells. Hepatitis B virus (HBV), belonging to Hepadnaviridae family, remains undetected in early infection as it does not induce the innate immune response and is known to be the cause of several hepatic diseases leading to cirrhosis and hepatocellular carcinoma. The association of PML-NB proteins and HBV is being addressed in a number of recent studies. Here, we report that the PML-NB protein Speckled 110 kDa (Sp110) is SUMO1-modified and undergoes a deSUMOylation-driven release from the PML-NB in the presence of HBV. Intriguingly, Sp110 knockdown significantly reduced viral DNA load in the culture supernatant by activation of the type I interferon-response pathway. Furthermore, we found that Sp110 differentially regulates several direct target genes of hepatitis B virus protein X (HBx), a viral co-factor. Subsequently, we identified Sp110 as a novel interactor of HBx and found this association to be essential for the exit of Sp110 from the PML-NB during HBV infection and HBx recruitment on the promoter of these genes. HBx, in turn, modulates the recruitment of its associated transcription cofactors p300/HDAC1 to these co-regulated genes, thereby altering the host gene expression program in favor of viral persistence. Thus, we report a mechanism by which HBV can evade host immune response by hijacking the PML-NB protein Sp110, and therefore, we propose it to be a novel target for antiviral therapy.

Hepatitis B virus (HBV),[2] which belongs to the Hepadnaviridae family, is an enveloped virus having a partially double-stranded DNA genome and is the leading cause of liver disease, ranging from acute and chronic hepatitis to liver cirrhosis and hepatocellular carcinoma (HCC) (1). The HBV genome has four overlapping open reading frames (ORFs) that encode for different proteins as follows: the polymerase; the core antigen (HBcAg); the surface antigen (HBsAg); and the X protein (HBx) (2). Among these, HBx is a multifunctional viral cofactor that has a significant role in viral pathogenesis and carcinogenesis (3, 4). The viruses often manipulate the host-signaling pathways so that it can replicate and propagate its genetic material and suppress the cellular defense mechanisms, such as the activation of the immune response or apoptosis induction (5). HBx promotes transcription of the HBV genome, maintained as an extrachromosomal entity (6), by hijacking the cellular Cul4–DDB1 complex to target the Smc5/6 for degradation (7).

Promyelocytic leukemia (PML) bodies are nuclear sub-structures, which are constituted of ~80 proteins including PML, Speckled 100-kDa protein (Sp100), transcription factor p53, the histone acetylase and co-activator CBP, the tumor suppressor Rb, the Bloom syndrome helicase BLM, heterochromatin protein 1 (HP1), etc. As these proteins play a significant role in many crucial cellular pathways, PML-NBs are often targeted by the viral proteins (5).

The Speckled family of transcription factors (Sp100, Sp140, and Sp110) is an important class of PML-body residents, which have several isoforms and are critically involved in gene regulation and anti-viral response (8, 9). Sp110 (Speckled, 110 kDa) has mainly four transcript variants, of which isoform-c is the full-length protein. Sp110b, the truncated isoform (amino acid sequence 1–549, which is up to the SAND domain), is expressed ubiquitously in human tissues and represses retinoic acid receptor α (RARα) activity in the nucleus (9, 10). In contrast, Sp110c, detected specifically in human peripheral blood leukocytes and spleen, is known to activate RARα-mediated transcription (9, 10). Sp110 is reported to be associated with the hepatic veno-occlusive disease with immunodeficiency (VODI) (11), acute promyelocytic leukemia (8), and tuberculosis (12–16). A study showed that Sp110b interacts with hepatitis C virus core protein and gets relocalized from the nucleus to the cytosol (mainly near the endoplasmic reticulum

This work was supported in part by Research Grants titled Biomolecular Assembly, Recognition, and Dynamics (BARD) Project Grant 12-R&D-SIN-5.04-0103 by the Department of Atomic Energy, Government of India. The authors declare that they have no conflicts of interest with the contents of this article.

This article contains supplemental Figs. S1–S10 and Tables S1–S6.

[1] Recipient of a Ramalingaswami Fellowship provided by Department of Biotechnology (DBT), Ministry of Science and Technology. To whom correspondence should be addressed. Tel.: 91-33-2337-5345-49 (Ext. 3106); Fax: 91-33-2337-4637; E-mail: chandrima.das@saha.ac.in.

[2] The abbreviations used are: HBV, hepatitis B virus; PML-NB, promyelocytic leukemia nuclear body; HBx, hepatitis B virus protein X; IHC, immunohistochemistry; CHB, chronic hepatitis B-infected; NASH, non-alcoholic steatohepatitis; qRT, quantitative RT; TSA, trichostatin A; HCC, hepatocellular carcinoma; EBV, Epstein-Barr virus; ISG, interferon-stimulating gene; ISRE, interferon-stimulated response element.

membranes). This sequestration of Sp110b from the nucleus by the core activates retinoic acid receptor-mediated transcription, thereby causing sensitization to all-*trans*-retinoic acid-mediated cell death (10). Another group showed that Sp110b plays an important role in Epstein-Barr virus (EBV) gene expression and virion production by interacting with the EBV nuclear protein SM and promoting gene transcription and enhancing mRNA stability. Depletion in the Sp110b level diminishes the ability of SM to enhance EBV lytic mRNA expression (9). A recent bioinformatics study proposed that RSF1 (remodeling and spacing factor 1) and ATF7IP (activating transcription factor 7 interacting protein), which are reported to be involved in transcriptional regulation and function as a chromatin remodelers in association with viral proteins like hepatitis B virus X protein (HBx) and Epstein-Barr virus BRLF1/Rta protein, are two potential interactors of Sp110 (17, 18).

In this study, we show that Sp110 remains in SUMO-1-modified form and undergoes a deSUMOylation-driven exit from the nuclear bodies in the presence of HBV or more specifically the HBV-encoded co-factor HBx. Sp110 was found to deregulate the expression of a large number of host genes, and interestingly, a significant number of them were direct targets of HBx, which were mostly implicated in the transcription, replication, repair, and immune-response pathways. Furthermore, we identified Sp110 as a novel interactor of the viral co-factor HBx, which hijacks the host protein and exploits its chromatin-binding property to get recruited to the co-regulated genes. HBx, in turn, modulates the recruitment of its associated transcription co-factors p300/HDAC1 to those genes, thereby altering the host gene expression program in favor of viral persistence. Altogether, our study shows that the host protein Sp110 is one of the prime factors that is exploited by HBV and is crucial for the pathogenesis as its knockdown led to a dramatic viral elimination and therefore is a potential therapeutic target.

Results

Host factor Sp110 shows hyper-expression on HBV infection

Nuclear body protein Sp110 is implicated in transcription regulation and several human diseases. We observed an augmentation of Sp110 expression with ELISA in the serum of chronically infected HBV patient samples when compared with the normal uninfected samples ($n = 15$) (Fig. 1*A*). This result was consistent with immunohistochemistry staining of normal, non-alcoholic steatohepatitis (NASH) and chronic hepatitis B-infected (CHB) liver tissues ($n = 10$) with the anti-Sp110 antibody (Fig. 1*B*), where the positively stained area in CHB is ~6-fold higher than normal tissues. To understand the role of Sp110 during HBV infection, we have used the following two models: 1.3-mer HBV plasmid (subgenotype D3) transfection in HepG2 cells where the HBV genome is present extra-chromosomally; and HepG2.2.15, a stable HBV (subgenotype D3)-producing cell line that is used in several premier studies (19–21). The efficacy of the 1.3-mer HBV plasmid transfection was confirmed by Southern blot analysis (Fig. 1*C*) as per standard protocol (22) as well as nested PCR (amplifying the surface antigen region of the HBV genome) with the DNA extracted from the culture supernatant (supplemental Fig. S1). We found that Sp110 mRNA and protein expression increased upon 1.3-mer HBV transfection (Fig. 1, *D* and *E*), similar to the data from the patient samples. HepG2.2.15 also showed a significant increase in the expression of Sp110 when compared with its parental cell line HepG2 (Fig. 1, *G* and *H*). Thus, Sp110 has an increased expression independent of whether the HBV genome is present extra-chromosomally or in integrated form.

HBV leads to an alteration in the SUMOylation status of Sp110 and causes its cellular re-localization

In HepG2 cells, Sp110 was found to reside inside the PML-nuclear bodies and co-localized with Sp100 and PML, markers of the nuclear bodies (Fig. 2*A*). When Sp100 (which is essential for PML-NB formation) is silenced, Sp110 was observed to have lost its usual punctate distribution and was distributed throughout the nucleus (supplemental Fig. S2). Interestingly, in HepG2.2.15 cells, Sp110 was found to have a distribution similar to supplemental Fig. S2, although the distribution of Sp100 was unaltered (Fig. 2*B, panel I*). Staining with PML further confirmed the integrity of the nuclear body HepG2.2.15 (Fig. 2*B, panel II*). Therefore, unlike many other virus infections, HBV infection did not cause PML-NB disruption (as also shown in a recent study (23)); however, Sp110 was found to be released from the PML body.

Small ubiquitin-like modifier 1 (SUMO1) plays a critical role in PML-NB formation, and SUMOylation is known to target many proteins to different nuclear sub-compartments. Many PML body proteins, including other Sp100 family proteins Sp100, Sp140, have been reported to get SUMO1-conjugated (8, 24). Because, the SUMOylation site of Sp100 and Sp140 lies in their N-terminal region, which has almost 49% homology to that of Sp110 (Fig. 2*C*) (8), we speculated that Sp110 could get SUMOylated. We performed co-immunoprecipitation, and it was found that Sp110 gets extensively SUMOylated in HepG2 cells (Fig. 2*D*, *panel I*), but there is no association between SUMO1 and Sp110 in HepG2.2.15 cells (Fig. 2*D*, *panel II*). Similar observations were seen by confocal imaging of Sp110 and SUMO1 in HepG2 and HepG2.2.15 cells (Fig. 2*E*), where there is a noteworthy decrease of SUMO1 levels in the latter. Furthermore, we transfected broad-range SUMO-specific proteases for SUMO1/2/3, SENP1, and SENP2 in HepG2 cells, as the other SENP family proteins have a higher preference for SUMO2/3 (25). Overexpression of the deSUMOylases resulted in diffused distribution of Sp110 along with a reduction in PML body staining of SUMO1, as compared with untransfected cells, which have higher SUMOylation levels (Fig. 2*F*). However, the integrity of the PML body was not lost because no significant alteration of PML body puncta was observed on SENP1 or SENP2 overexpression (supplemental Fig. S3). Thus, it can be concluded that in HepG2 cells, Sp110 is present in PML bodies in a SUMOylated form. HBV leads to deSUMOylation of Sp110 and its consequent exit from the PML body.

Sp110 favors viral proliferation by regulating the type I IFN-response pathway genes

The increased expression of Sp110 and its differential distribution upon HBV infection indicated that it might be playing

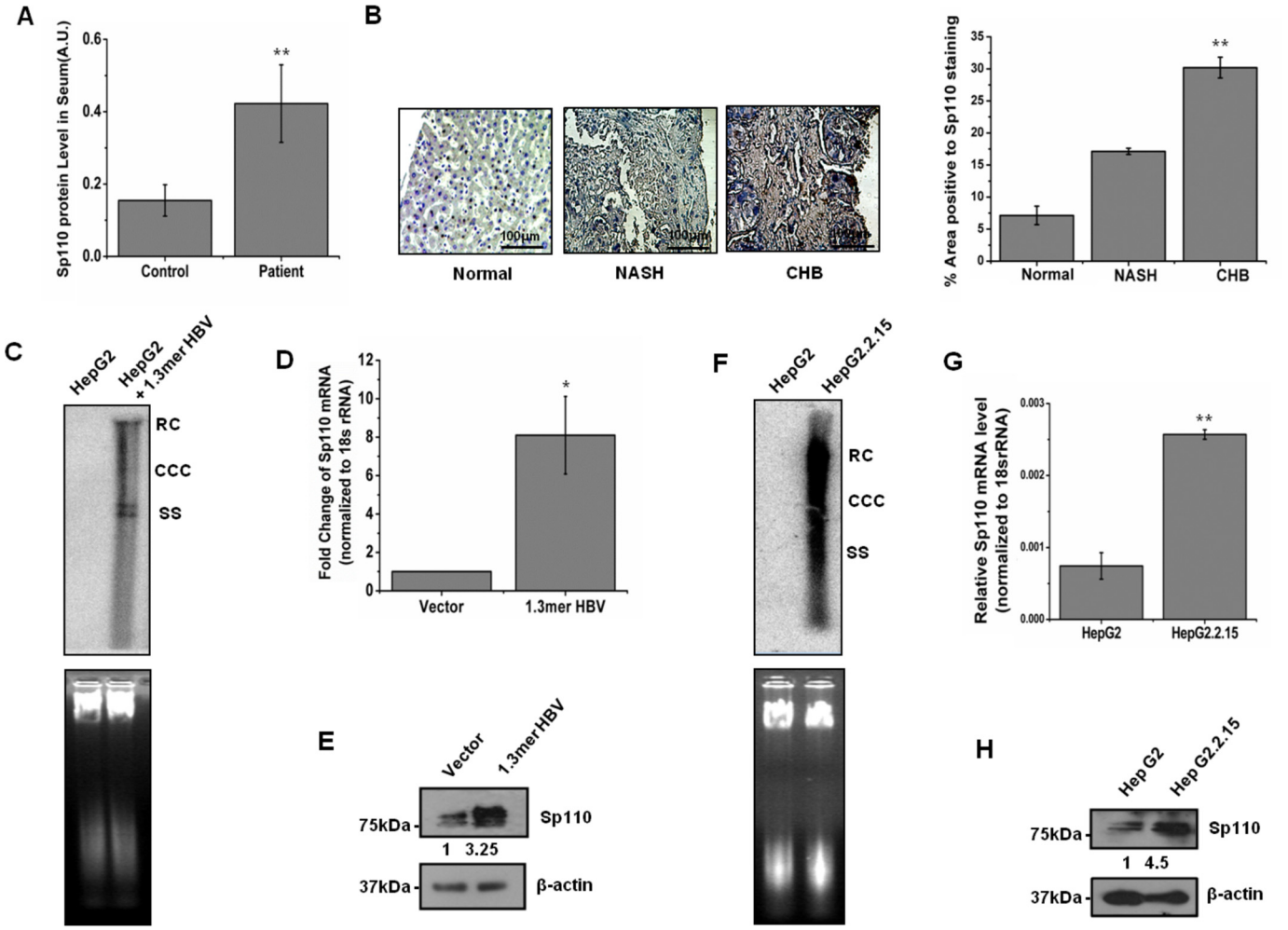

Figure 1. Sp110 hyper-expression upon HBV infection. *A,* increased expression of the Sp110 protein in normal and HBV-infected patient serum (having a viral load $>10^5$ copies/ml), quantified by ELISA, $n = 15$. *B,* immunohistochemistry staining of normal, NASH, and CHB liver tissues ($n = 10$) with anti-Sp110 antibody and quantification of the positively stained area also show a similar increase. *Scale bar,* 100 μm. *C,* Southern blot with DNA extracted from HepG2 with or without 1.3-mer HBV plasmid transfection confirms that viral production and thus the effectiveness of the transfection. Relaxed circular double-stranded (*RC*), covalently closed circular DNA (*CCC*), and single-stranded (*SS*) are the various HBV DNA replicative intermediates shown. The agarose gel image shows comparable loading of total DNA. *D* and *E,* relative expression of Sp110 in HepG2 cells on 1.3-mer HBV transfection at mRNA level by qRT-PCR (*D*) and protein level by Western blotting and quantification (*E*) show a significant increase. *F,* Southern blot with the DNA isolated from the of HepG2.2.15 cells confirms the viral production. *G* and *H,* Sp110 mRNA (*G*) and protein expression quantified (*H*) in HepG2.2.15 cells show a similar increase. Data are represented as mean ± S.D. from at least three independent experiments. The statistical significance has been represented as follows: **, $p < 0.01$; *, $p < 0.05$.

some crucial function. To understand whether Sp110 has a direct role to play in the infection, we silenced Sp110 in HepG2.2.15 cells and scored the viral DNA load. Sp100, another PML-NB body, has been used as a control. The efficacy of Sp110 and Sp100 knockdown was confirmed by Western blotting (Fig. 3*A*). We observed that Sp110 silencing led to a dramatic reduction of viral DNA load although no significant change was observed upon Sp100 knockdown (Fig. 3*B* and supplemental Fig. S4*A*). A diminution of the viral DNA was also detected by Southern blot analysis (Fig. 3*C*) as well as nested PCR from the culture supernatant (supplemental Fig. S1). The decrease was also evident in viral protein HBsAg levels (supplemental Fig. S4*B*). Previous studies have shown that HBV inhibits apoptosis to release infectious progeny, and HBV proteins play a major role in it by blocking the caspase-independent apoptosis pathway (26, 27). Because viral elimination was observed upon Sp110 knockdown, we were interested in looking into its effect on the apoptosis repression. The flow cytometric data upon Sp110 silencing showed a substantial increase in the sub G_0 cell population (Fig. 3*D* and supplemental Fig. S5) indicating cell death. Observations with the APOSTRAND^{TM} kit, which detects the apoptotic DNA levels, in a sample confirmed that Sp110 knockdown indeed makes the cell more apoptosis-prone (Fig. 3*E*), suggesting an anti-apoptotic role of Sp110 during HBV infection. This corroborates a decrease in cell viability (Fig. 3*F*) and mRNA expression of proliferation marker genes (Ki-67, MCM2, PCNA, and BCL2) (Fig. 3*G*).

Microarray analysis was done for Sp110 silenced compared with negative control silenced Hep2.2.15 cells to understand its role in HBV infection. The heat map with an absolute fold-change cutoff of 1.5 is shown in Fig. 4*A*. About 890 genes belonging to different cellular processes were found to be differentially regulated (absolute fold-change ≥ 1.5 and $p \leq 0.05$) (supplemental Table S3), which were grouped through the Significant Biology Network (Fig. 4*B*). By further analyzing the total differentially expressed gene set at a higher stringency

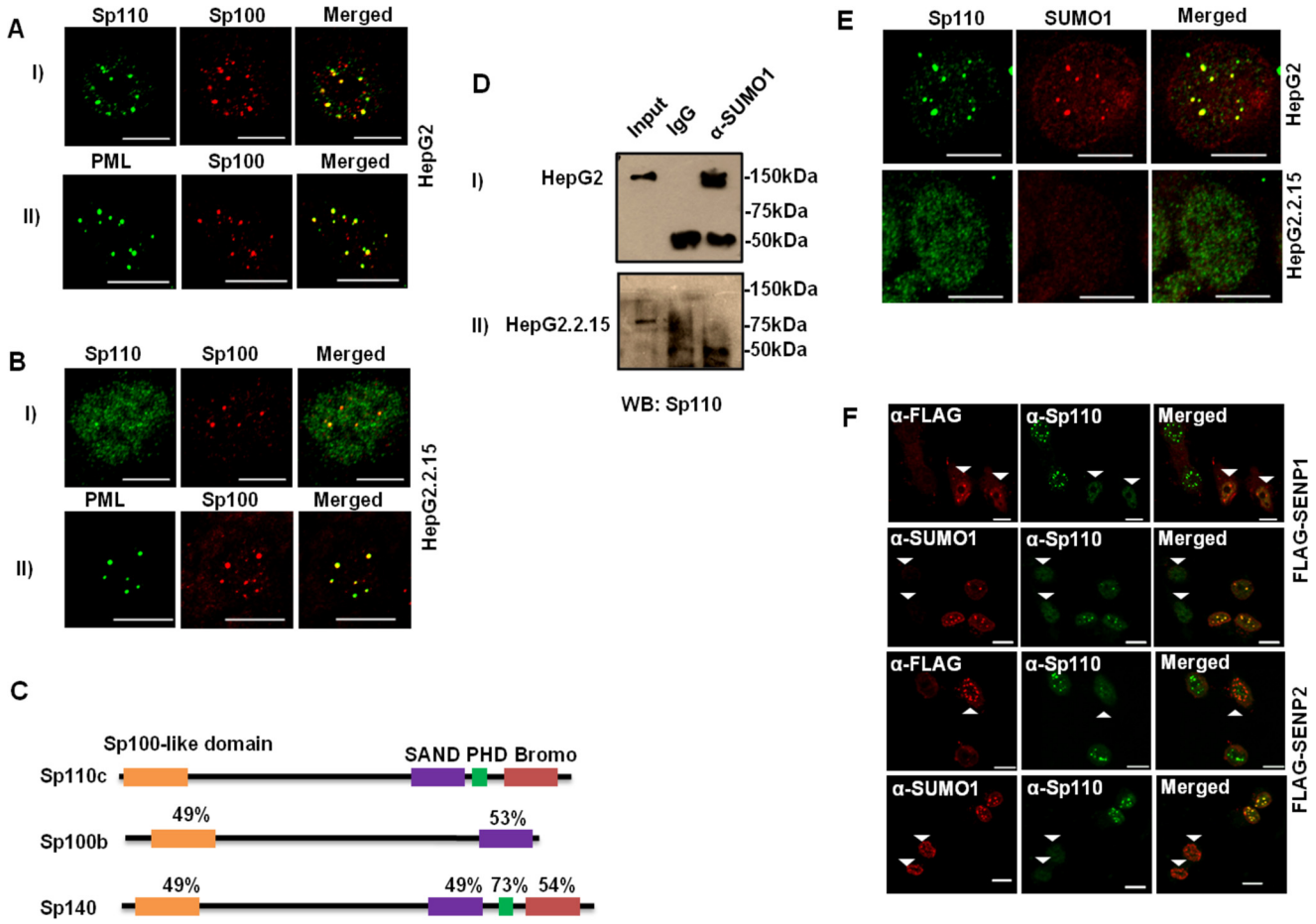

Figure 2. Differential distribution of Sp110 in absence and presence of HBV due to its SUMO1 modification and deSUMOylation triggered release from PML-NB. *A,* co-immunofluorescence staining of Sp110 (Alexa 488) with Sp100 (Alexa 594) (*panel I*) and PML (Alexa 488) with Sp100 (Alexa 594). *Panel II* shows that Sp110 remains within the PML body in HepG2 cells. *B,* co-immunofluorescence staining of Sp110 (Alexa 488) with Sp100 (Alexa 594) (*panel I*) and PML (Alexa 488) with Sp100 (Alexa 594) (*panel II*) in HepG2.2.15 cells. Differential distribution of Sp110 and co-localization of PML and Sp100 indicate that the PML bodies are not disrupted in the presence of HBV, but Sp110 is released from its usual niche. *C,* comparative schematic representation of the domains of Sp110 with other Sp100 family proteins. The percentage homology of Sp110 to the corresponding regions is mentioned as reported previously (8). *D,* co-immunoprecipitation with α-SUMO1 antibody, followed by immunoblotting with the α-Sp110 antibody. Sp110 was found to be modified by SUMO1 in HepG2 (*panel I*) in contrast to HepG2.2.15 (*panel II*). *E,* immunofluorescence staining of Sp110 (Alexa 488) and SUMO1 (Alexa 594) shows that the SUMO1 is significantly present in the PML bodies in HepG2 but not in HepG2.2.15 cells. *F,* immunofluorescence staining of Sp110 (Alexa 488), FLAG (Alexa 594) and SUMO1 (Alexa 594). Overexpression of SUMO-specific proteases FLAG-SENP1 and FLAG-SENP2 in the cells (indicated by *arrow*) results in the decrease of SUMO1 levels in the cells and a loss of the punctate pattern distribution of Sp110, indicating that Sp110 release from the PML body is triggered by its deSUMOylation (supplemental Fig. S3; which shows that deSUMOylase overexpression does not change the PML body integrity). The *scale bar,* 10 μm. The experiments were repeated at least three times independently.

(absolute fold-change ≥ 2.0; $p \leq 0.05$; minimum required interaction score 0.7, high confidence) by STRING database (28), we obtained a network hub consisting of IFN regulatory factor 9 (*IRF-9*), signal transducers, and transactivator 1 (*STAT1*), 2′-5′-oligoadenylate synthetase 1 (*OAS1*), *OAS3*, IFN-induced proteins with tetratricopeptide repeats 1 (*IFIT1*), *IFIT3*, interferon-α-inducible protein 27 (*IFI27*), *IFI6*, myxovirus resistance 1 (*Mx1*), etc., which are classical components of the type I interferon-response pathway (Fig. 4*C* and supplemental Table S4). The up-regulation of all these genes upon Sp110 silencing was validated by qRT-PCR (Fig. 4*D*). On a closer look, these genes were found to be either a component of or the target of transcription factor ISGF3 (a hetero-trimeric complex of STAT1, IRF9, and STAT2, which plays a crucial role in the IFN-I-response pathway). The increased expression of the ISGF3 factors was detected by Western blotting (Fig. 4*E*), which probably explains the up-regulation of its downstream targets.

Previous studies reported that trichostatin A (TSA) inhibits the type I interferon pathway by blocking the formation of the ISGF3 factor thus affecting the activation of the downstream interferon-stimulating genes (ISGs) (29, 30). We found that concomitant TSA treatment along with Sp110 knockdown in HepG2.2.15 cells did not show the viral abolition by qRT-PCR (Fig. 4*F*) and Southern blotting (Fig. 4*G*), thereby confirming that the type I interferon-response pathway activation plays a crucial role in observed viral elimination. Because TSA blocks the ISGF3 formation and the network hub obtained consisted of ISGF3 components and its downstream targets, we were interested in looking into their regulation by Sp110. In this context, we were interested to identify the role of full-length Sp110c isoform, for which the subsequent experiments were performed by overexpressing FLAG-Sp110c. The chromatin association of FLAG-Sp110c was confirmed by chromatin fractionation assay (supplemental Fig. S6). We observed that the

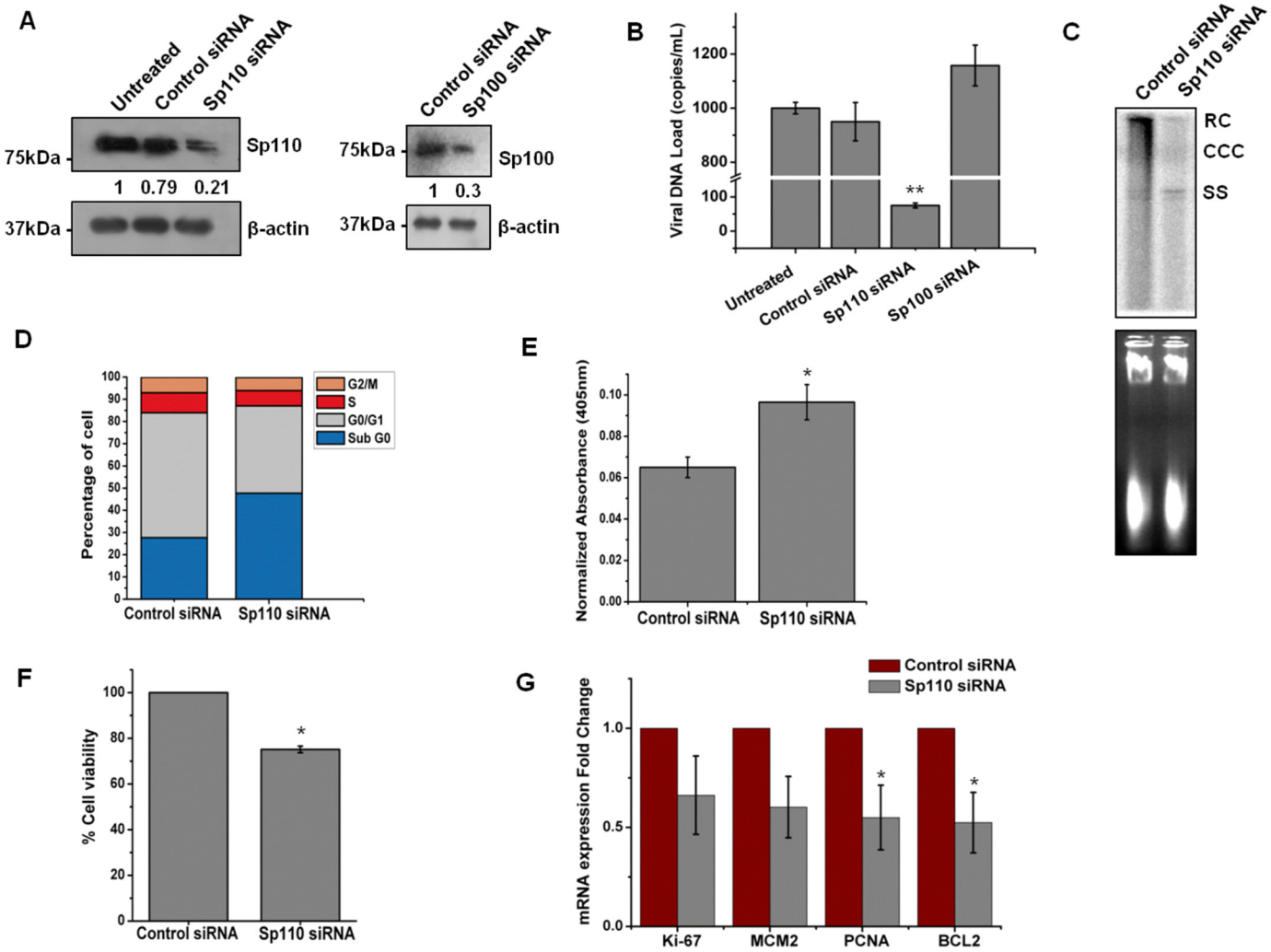

Figure 3. Sp110 knockdown leads to viral elimination and apoptosis induction. *A,* Sp110 and Sp100 silencing verified by Western blotting. *B,* drastic decrease in the amount of HBV DNA released in the culture supernatant (viral load) was observed upon Sp110 silencing, but no significant change was observed upon Sp100 knockdown. *C,* Southern blot for the DNA isolated reconfirms the reduction in the viral DNA release upon Sp110 silencing. Relaxed circular double-stranded (*RC*), covalently closed circular DNA (*CCC*), and single-stranded (*SS*) are the various HBV DNA replicative intermediates shown. The agarose gel image shows comparable loading of total DNA. *D,* quantification of FACs profiles (supplemental Fig. S5) representing the percentage of cell in each cell-cycle phase; the increase in the sub-G_0 population indicates significant cell death on Sp110 knockdown. *E,* ELISA-based detection showing an increased number of apoptotic cells in HepG2.2.15 Sp110 siRNA when compared with control siRNA samples. *F,* 3-(4,5-dimethylthiazol-2-yl)-2,5-diphenyltetrazolium bromide assay showing decreased cell viability on Sp110 knockdown. *G,* relative mRNA expression of proliferation marker genes (Ki-67, MCM2, PCNA, and BCL2) upon Sp110 silencing shows reduction, indicating a reduced proliferation. The data are represented as mean ± S.D. from three independent experiments. Statistical significance has been represented as follows: **, $p < 0.01$; *, $p < 0.05$.

mRNA level of the genes showed a significant decrease upon Sp110c overexpression (Fig. 4*H*), and ChIP assays confirmed that there is a direct recruitment of Sp110c to the promoters of *IRF9, STAT1,* and *STAT2* (Fig. 4*I*) in HepG2.2.15 cells. Furthermore, luciferase assay with 1.3 kb from the *STAT1* promoter region cloned in the pGL3-basic vector showed significant repression on the presence of Sp110 (Fig. 4*J*). Thus, our results show that host factor Sp110 regulates the type I interferon-response pathway, which has direct implication in viral elimination.

Sp110 affects the recruitment of viral protein HBx to the promoters

HBx is a crucial factor that is responsible for viral pathogenesis (31). It is known to utilize the host cellular machinery for reprogramming the host gene expression network, leading to tumorigenicity (32). Comparison of Sp110 silenced microarray data (supplemental Table S3) with the integrated ChIP-chip, and microarray data of HBx (33) revealed that a significant number of genes, which are direct targets of HBx, were differentially regulated by Sp110 (supplemental Table S5). Most of these genes were found belonging to the following pathways: immune response, signaling, metabolism, transcription, replication, and DNA repair (Fig. 5*A* and supplemental Table S6). The network of the mentioned pathways has been shown in Fig. 5*B*. Apart from these, many microRNA targets were obtained from the comparative analysis (data not shown). Few candidate genes of the selected pathways were subsequently validated (Fig. 5*C*). Because Sp110 silencing differentially regulated a substantial number of target genes of HBx but did not significantly alter the expression of the latter (Fig. 5*D* and supplemental Fig. S7*A*), we hypothesized that it is probably the HBx recruitment to these

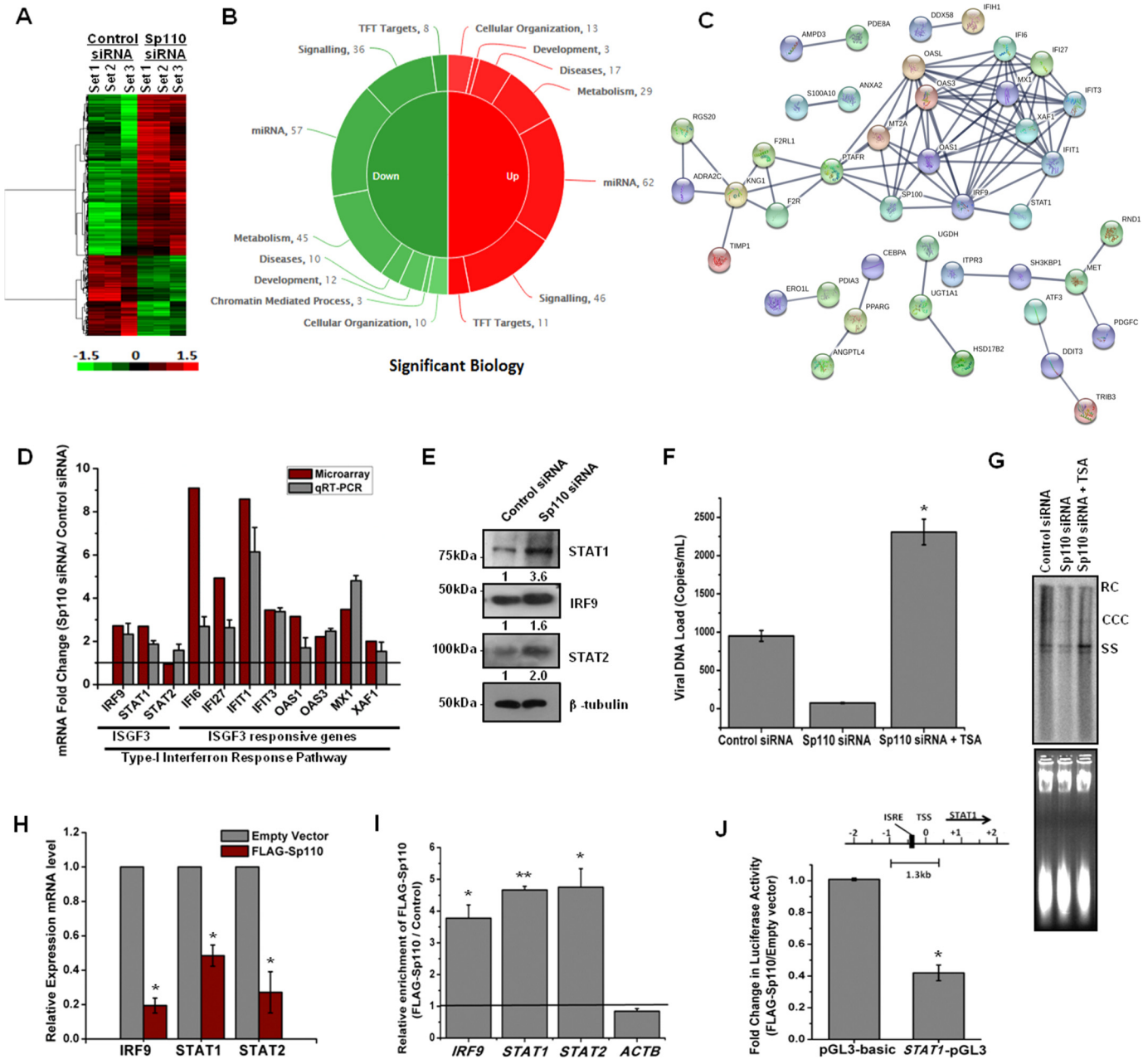

Figure 4. Sp110 regulates type I IFN-response pathway. *A,* heat map representation of microarray data for HepG2.2.15 control siRNA and Sp110 siRNA samples. *B,* differentially regulated genes, grouped into different biological processes through the significant biology network. Cut offs for the gene selections were $-1.5 >$ fold-change > 1.5, and a p value <0.05. *C,* network obtained from STRING network analysis of differentially regulated genes (absolute fold-change ≥ 2.0; $p \leq 0.05$; minimum required interaction score: 0.7, high confidence) revealed a hub of highly connected nodes, belonging to the type I interferon-response pathway. The network is based on interactions reported experimentally, in databases or proteins that are co-expressed. *D,* validation of some of the genes obtained from type I interferon-response pathway by qRT-PCR. *E,* Western blot and quantification of for the ISGF3 factors, STAT1, STAT2, and IRF9 show an increase in expression upon Sp110 silencing. *F* and *G,* relative viral DNA load on treatment with 300 nM of TSA for 16 h. Addition of TSA reversed the observed decrease in viral load upon Sp110si as detected by qRT-PCT (*F*) and Southern blot (*G*). Relaxed circular double-stranded (*RC*), covalently closed circular DNA (*CCC*), and single-stranded (*SS*) are the various HBV DNA replicative intermediates shown. The agarose gel image shows comparable loading of total DNA. *H,* repression of transcription of the ISGF3 factors upon Sp110c overexpression. *I,* ChIP shows Sp110c recruitment on *IRF9, STAT1,* and *STAT2* promoters. *J,* luciferase assay with *STAT1* promoter region cloned in pGL3-basic vector showed significant repression on the presence of Sp110. The data are represented as mean ± S.D. from three independent experiments. Statistical significance has been represented as follows: **, $p < 0.01$; *, $p < 0.05$.

genes that is being affected by Sp110. We indeed found a noteworthy decrease in HBx recruitment in candidate genes *MYCN, TAF5, PERP,* and *BCL2L12* upon Sp110 silencing (Fig. 5*E*), whereas *ACTB*, used as a negative control, did not show any change in the recruitment on Sp110 knockdown. Previous reports have shown that HBx associates with transcriptional co-activator (p300)/co-repressor (HDAC1) and alters the epigenetic landscape near its target genes thereby affecting the host gene expression (34, 35). We found that reduced recruitment of HBx in the absence of Sp110 also altered the enrichment of its p300/HDAC1 at the targets (although their expression remains unaltered, supplemental Fig. S7*B*). A reciprocal recruitment of p300 and HDAC1 was observed at the similar sites (Fig. 5, *F* and *G*), which resulted

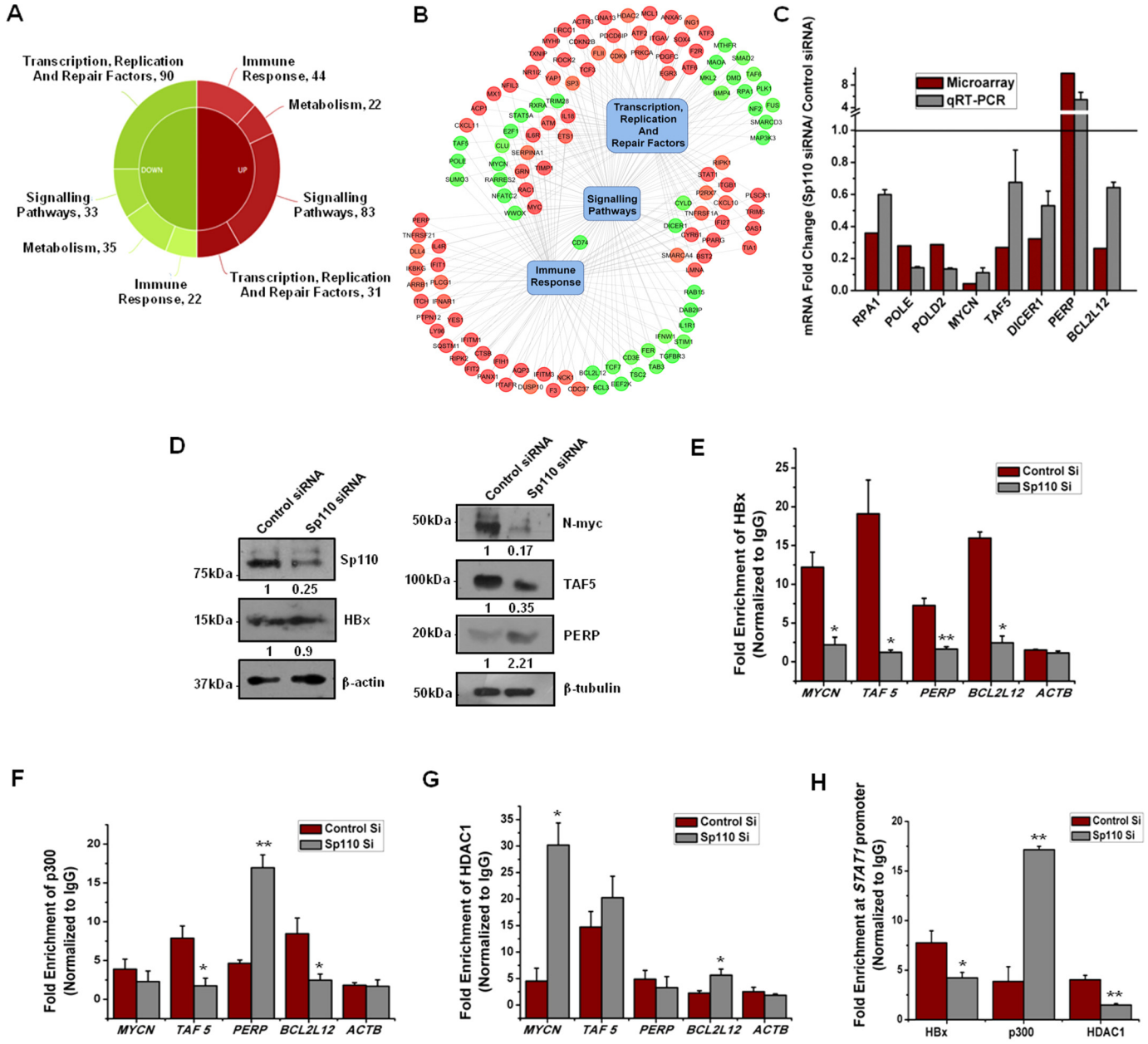

Figure 5. Substantial overlap between Sp110-deregulated genes and direct targets of HBx is implicated in immune response, transcription, replication, and repair. Sp110 can influence transcription of these genes by altering HBx recruitment, thereby modifying p300/HDAC1 distribution. *A,* Sp110-HBx co-regulated genes grouped into different biological processes that are significantly altered. Signal intensity cutoff >1.5 for HBx recruitment on the genes from ChIP-on-chip data analysis and an absolute fold-change >1.2 for HBx and Sp110 microarray. *B,* network analysis of Sp110 deregulated HBx direct target genes in pathways associated with viral infection. *C,* differential expression of co-regulated gene candidates from replication, transcription regulation, and apoptotic pathway upon Sp110 knockdown were validated by qRT-PCR. *D,* immunoblots showing alteration in expression of HBx target genes N-myc, TAF5, and PERP, whereas the expression of HBx remains almost unaltered upon Sp110 knockdown host factors. *E,* ChIP assay showed significantly decreased recruitment of HBx from its target gene promoters upon Sp110 silencing in HepG2.2.15 cells. *MYCN, TAF5, BCL2L12,* and *PERP* are HBx regulated genes, and *ACTB* is the negative control. *F* and *G,* fold-change in the enrichment of p300 (*F*) and HDAC1 (*G*) on promoters of HBx-regulated genes in HepG2.2.15 Sp110 silenced over control silenced cells. Lack of HBx from the target sites therefore affects the recruitment of the transcriptional co-activators/co-repressors known to be associated with it, thereby altering the expression of the target genes. Up-regulated genes like *PERP* have increased enrichment of p300 and decreased recruitment of HDAC1 in their promoter on Sp110 silencing, and the reverse is true for down-regulated genes like *MYCN, TAF5,* and *BCL2L12*. *ACTB* is the negative control, which remains unaltered upon Sp110 knockdown. *H,* type I interferon-response gene *STAT*1 is co-regulated by Sp110 and HBx by a similar mechanism. All the data are represented as mean ± S.D. from at least three independent experiments. Statistical significance has been represented as follows: **, $p < 0.01$; *, $p < 0.05$.

in their differential transcription. The promoters of down-regulated genes, *MYCN, TAF5,* and *BCL2L12*, were found to have a higher occupancy of HDAC1 and a lower occupancy of p300 while the promoter of up-regulated gene *PERP* had a higher p300 recruitment and lower HDAC1 recruitment. Interestingly, some of the interferon type I pathway candidates (*STAT1, IFI27, IFIT1, IFIT2, OAS1,* and *MX1*) were also prominent hits in the HBx-Sp110 co-regulated network, and we observed a similar mode of recruitment of HBx at the *STAT1* promoter, which was previously found to be a direct Sp110 target (Fig. 5*H*). Thus, Sp110 directly or indirectly helps in HBx recruitment leading to alteration in the epigenomic landscape, which favors viral persistence.

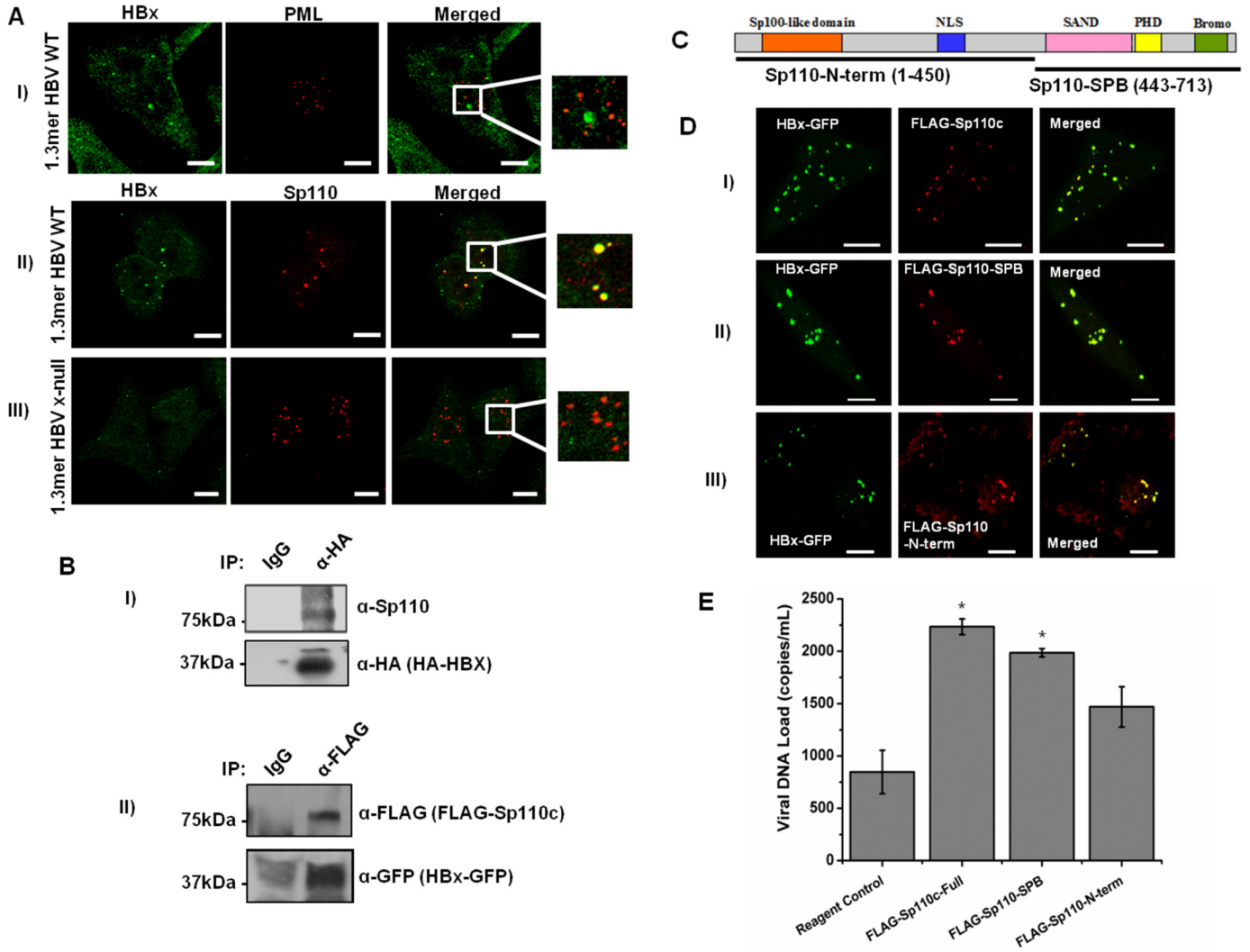

Figure 6. HBx shows cooperative association with Sp110 and drives it out of the PML-NB. *A,* co-immunofluorescence staining showing that Sp110 associates with HBx to exit the PML-NBs (*panel I*) shows HBx (Alexa 488) does not co-localize with PML-NBs, stained with its marker protein PML (Alexa 594). *Panel II* shows the usual PML-NB distribution of Sp110 (Alexa 594) altered upon 1.3-mer HBV transfection, and Sp110 co-localizes with HBx. *Panel III* shows Sp110 remains in its PML-NB distribution upon 1.3-mer HBV X-null transfection. *B, panel I,* co-immunoprecipitation with α-HA antibody in HA-HBx-transfected HepG2 cells, followed by immunoblotting with a α-Sp110 antibody, confirms the interaction between HBx and Sp110. *Panel II,* co-immunoprecipitation with α-FLAG antibody in HepG2 cells co-transfected with GFP-HBx and FLAG-Sp110c, followed by immunoblotting with α-GFP antibody, validated the interaction. *C,* schematic representation of the domain organization in Sp110. *D,* immunofluorescence staining of HBx-GFP and α-FLAG (Alexa 594) to show HBx co-localizes with both FLAG-Sp110c-full (*panel I*) and FLAG-Sp110-SPB (*panel II*) (Pearson's coefficient 0.60 ± 0.054 and 0.71 ± 0.082, respectively) and partially co-localizes with FLAG-Sp110-N-term (*panel III*) (Pearson's coefficient 0.38 ± 0.081). *Scale bar,* 10 μm. *E,* overexpression of FLAG-Sp110 and FLAG-Sp110-SPB or in HepG2.2.15 cells results in a significant increase in the HBV viral DNA load. FLAG-Sp110-N-term overexpression also increases the viral load but to a comparatively lesser extent. The experiments were independently repeated at least three times and for co-localization studies, $n = 20$. All the data are represented as a mean ± S.D. The statistical significance has been represented as follows: **, $p < 0.01$; *, $p < 0.05$.

Viral co-factor HBx interacts with host factor Sp110 and drives it out of the PML-NB

Because we found that recruitment of HBx on the target promoters is dependent on Sp110, we hypothesized that both the proteins were a part of the same transcriptional complex. From immunofluorescence staining of 1.3-mer HBV plasmid-transfected HepG2 cells, we observed that PML does not co-localize with HBx (Fig. 6*A*, *panel I*) but Sp110 (Alexa 594) distribution changes from its usual PML-NB niche and co-localizes with HBx (Fig. 6*A*, *panel II*). On the contrary, upon transfection of 1.3-mer HBV X-null plasmid, Sp110 remains in its usual PML-NB distribution (Fig. 6*A*, *panel III*), suggesting that HBx is responsible for relocalization of Sp110. HBV core protein staining (Alexa 488) (supplemental Fig. S8) indicated a comparable transfection efficiency for 1.3-mer HBV and 1.3-mer X-null HBV plasmids. We had a similar observation by overexpressing HBx, where Sp110 was released from the PML-NBs to co-localize with HBx (Pearson's coefficient 0.86 ± 0.091) (supplemental Fig. S9). Subsequently, co-immunoprecipitation (co-IP) in HBx-overexpressed cells (Fig. 6*B*) as well as 1.3-mer HBV-transfected cells (supplemental Fig. S10) confirmed that HBx had a significant association with Sp110. Further investigation showed that SENP1 (but not SENP2) possibly is a part of the Sp110-HBx co-complex (supplemental Fig. S9), indicating the deSUMOylation-driven exit of Sp110 and its interaction with HBx are probably a concerted process.

Immunofluorescence studies of HepG2 cells co-transfected with HBx-GFP and FLAG-Sp110c (full) and FLAG-Sp110-SPB

or FLAG-Sp110-N-term (Fig. 6*D*) showed that HBx had a better co-localization with the full-length (Pearson's coefficient 0.60 ± 0.054) and SPB module (the chromatin-binding region harboring the SAND, PHD, and Bromodomain) of the protein (Pearson's coefficient 0.71 ± 0.082), when compared with the N terminus (Pearson's coefficient 0.38 ± 0.081). Interestingly, it was observed that overexpression of the full-length and SPB module resulted in a dramatic increase in viral DNA load in the culture supernatant, whereas the N-terminal construct showed only a partial increase (Fig. 6*E*). These results show that the chromatin-binding module of Sp110 is more actively involved in its association with HBx as well as in its contribution to viral persistence, which corroborates with our previous results where the host protein was found to influence the recruitment of HBx. Therefore, it can be interpreted that HBx, which does not harbor any DNA-binding module (33), probably exploits the chromatin-binding property of Sp110 (supplemental Fig. S2) to be recruited to its target site and maintain sustained viral proliferation in host cells.

Discussion

Several DNA and RNA viruses have been reported to exploit resident factors of PML bodies, which occur by mainly two distinct mechanisms: (i) some of the viral proteins associate with PML body proteins leading to disruption of the sub-nuclear compartment, and (ii) the viral genome of few DNA viruses can associate with the PML nuclear body, which might contribute toward viral proliferation (5). Hepatitis B virus, a Hepadnaviridae family virus, is the cause of many chronic hepatic diseases leading to cirrhosis and hepatocellular carcinoma, but the association of HBV and the PML-NBs are not much explored. PML body resident protein p11, an S100 family member, has been reported to associate with HBV polymerase inside the PML body favoring viral replication (36), whereas knockdown of the PML gene leads to increased viral replication thereby causing HBV-induced HCC (37, 38). A recent study showed that smc5/6 restricts viral transcription when localized in the PML body (23).We found that transcription factor Sp110, a nuclear body resident protein, shows a selective exit from the PML body upon infection and is hijacked by HBx to promote viral proliferation. This indicates that the residents of PML-NBs have distinct roles in HBV infection.

Previous studies have shown that SUMO1 is a crucial regulator of various signaling pathways and is also involved in the formation of the PML body and the dynamic organization of the protein complexes in there (39). PML-NB proteins remain sequestered and are released following a cue from its environment, like STAT3, which remains sequestered in the PML body and is released upon IL-6 treatment, due to SENP1-mediated deSUMOylation of the PML (40). SENP1 was also found to cause dissociation of homeodomain-interacting protein kinase 2 (HIPK2) from the PML body (41). Furthermore, in rheumatoid arthritis synovial fibroblasts, hyper-expression of SUMO1 is observed, which causes increased SUMOylation and recruitment of transcriptional repressor DAXX to the PML body, resulting in Fas-induced apoptosis resistance of the cells. Overexpression of deSUMOylase SENP1 has been shown to revert the effect of SUMO1 by releasing DAXX from the nuclear body to carry out its proapoptotic functions (42). These reports highlight the importance of the SUMOylation and deSUMOylation switch in the proper functioning of the cell. Sp110, being a PML-NB resident and an Sp100 family protein, can be predicted to be associated with SUMO1. Here, we show that indeed Sp110, like other PML body proteins, remains SUMO1-modified inside the PML-NBs, and its deconjugation from SUMO causes Sp110 to exit the nuclear subcompartment. Such a deSUMOylation triggered re-localization of Sp110 that was observed during HBV infection. Interestingly, this re-localization could be observed only in the presence of HBx, which was found to interact with Sp110. Moreover, HBx on overexpression co-localized specifically with deSUMOylase SENP1 and not SENP2, indicating that Sp110, HBx, and SENP1 are possibly part of the same complex, thereby suggesting that association of Sp110 with HBx and its deSUMOylation to be concerted steps.

HBx, a multifunctional co-factor of HBV, interacts with several host factors promoting HBV replication. For example, it hijacks the cellular Cul4–DDB1 complex to target the intrinsic antiviral restriction factor Smc5/6 for degradation (7, 23). It is also reported to interact with the cellular oncoprotein RMP (RNA polymerase II subunit 5-mediating protein) to inhibit the expression of apoptotic factors and promote proliferation, thereby leading to hepatocarcinogenesis (43), whereas its interaction with protein kinase BubR1 and HBx causes dysregulation of the mitotic checkpoint resulting in chromosomal instability, frequently observed in HBV-induced HCC (44). While being a dynamic co-factor, HBx lacks a DNA-binding domain of its own and is often reported to be recruited to gene promoters via host transcription factors like p53, YY1, E2F1, etc. (33, 45). In this study, we identified Sp110 as a novel interactor of HBx. The viral protein was found to hijack and exploit the chromatin-binding property of Sp110 to be recruited to several of its host target genes. HBx, in turn, can recruit its associated transcription co-activator– co-repressor complexes to the loci thereby leading to host gene expression reprogramming in favor of viral proliferation.

Previous reports show that HBV acts as a stealth virus in early infection as it does not induce the innate immune response, the first line of defense against viral infection, and thus remains undetected (46, 47). A recent study further confirmed that HBV does not invoke the interferon signaling in primary human hepatocytes (23). Interferon-α is a well-approved treatment for HBV infection, but still, it rarely cures the disease, primarily because HBV interferes with the IFN signaling. Although the mechanism is not well explored, HBV polymerase protein has been reported to inhibit the IFNα-signaling pathway leading to persistence of HBV (48). In this study, we observed that Sp110 silencing in HBV-producing cells resulted in viral abolition accompanied by increased apoptosis and decreased cell viability. On transcriptional analysis, we found a broad range of host gene expression alterations, including core transcription machinery, metabolism, and cell-signaling pathway, but the maximum differential expression was observed for the type I IFN-response pathway genes, which were highly up-regulated. Moreover, because the expected viral elimination was not witnessed upon concomitant treatment of trichostatin A (previously reported to inhibit ISGF3 formation) (29), the type I IFN-

response pathway can be interpreted to have a crucial role in it. The other altered signaling and metabolic and pathway genes may also have a direct or indirect effect on the viral gene expression and need further study. Furthermore, we confirmed that Sp110 regulates the interferon I-response pathway, and the components of the ISGF3 factor, STAT1, IRF9, and STAT2, are direct targets of Sp110. Because we found that knocking down the host factor leads to activation of ISGs, we propose that Sp110 could be a potential target for the antiviral therapy, which could bypass the shortcomings of interferon-α treatment.

We subsequently performed a systematic classification of genes and found that Sp110 silencing can differentially regulate a large class of genes that are HBx targets and could be subgrouped in three broad categories: transcription, replication, and repair factors; signaling pathway proteins; and factors that modulate host immune response. As Sp110 and HBx can have both transcription activation and repression function (8, 10, 32), some co-regulated direct target genes showed up-regulation in the absence of Sp110, whereas the others underwent down-regulation. We observed that the transcription of a large number of factors promoting (i) replication like POLE, POLD1, POLD2 (subunits of DNA polymerase), and RPA1 (replication protein 1A); (ii) transcription like POLR2I and POLR2J (subunits of RNA polymerase), GTF2F2 (general transcription factor IIF subunit 2), TAF5, and MYCN; and (iii) post-transcriptional processing like DICER are significantly down-regulated upon Sp110 silencing. The expression of some of these important factors have been validated by qRT-PCR. We subsequently observed a significant reduction in HBx recruitment into some of these candidate genes upon Sp110 silencing, which suggests us that Sp110 and HBx might be having an activation function on these genes to promote proliferation, thereby inducing carcinogenesis.

In contrast, most of the type I interferon-response genes, which were up-regulated upon Sp110 silencing, were also found to be direct targets of HBx. We propose that Sp110 is involved in maintaining the repressed state of these genes by helping in the recruitment of HBx, which subsequently brings HDAC1. Sp110 and HBx directly regulate ISGF3 factor component STAT1 and downstream ISGF3-responsive genes like *IFI27, IFIT1, OAS1,* and *MX1*. ISGF3 is a vital transcription factor in the JAK-STAT pathway, which activates the transcription of downstream ISGs by binding to the interferon-stimulated response element (ISRE) in their promoters (50). Moreover, ISGF3 was also found to interact with an ISRE-like sequence in the enhancer element EnI of the HBV genome to mediate its suppression and modulate HBV replication (51). The higher expression of ISGF3 components due to Sp110 knockdown causes induction of the downstream ISGs, which accomplish their anti-viral activity through different pathways. For example, OAS1 synthesizes 2′,5-oligoadenylates, which activate latent RNase L and thus causes viral RNA degradation and inhibition of viral replication (52). MxA (human homolog of mouse Mx1), an interferon-induced dynamin-like GTPase, interacts with HBcAg, which causes the immobilization of the latter in the perinuclear structures and subsequently prevents the nucleocapsid formation (53, 54). In contrast, IFIT1, strongly induced by type I IFN, suppresses cellular translation by binding to the translation initiator eIF3 subunits (55, 56) and was shown to block viral replication by the sequestration of pppRNA (5′-triphosphate RNA) (57). Furthermore, it was found that siRNA-mediated silencing of IFIT1 caused a dramatic amplification of viral replication and the reciprocal situation upon IFIT1 overexpression (58), which supports our data as Sp110 silencing up-regulates IFIT1. Therefore, it can be envisaged how the differential expressions of the important host factors due to reduced recruitment of HBx in the absence of Sp110 have significant contributions in viral elimination.

Taken together, our study identified a novel mechanism by which HBV can evade the host immune-response pathway. We show for the first time that host factor Sp110, which is usually a PML-NB resident, is hijacked and exploited by HBx to reprogram the host transcription network favoring viral persistence. Thus, Sp110 plays a crucial role in viral pathogenesis. Although we identified the role of Sp110 in the regulation of HBV infection, it is important to note that this host factor also has HBV-independent cellular functions, as evident from its gene targets, whose underlying mechanisms have yet to be elucidated. Nevertheless, considering a diversity of functions that Sp110 can play during HBV pathogenesis, we speculate that Sp110 can be a next generation therapeutic target.

Experimental procedures

Cell culture conditions, overexpression, and siRNA transfection

HepG2 cells (human hepatoblastoma cell line) were maintained in Dulbecco's modified Eagle's medium (Gibco, Invitrogen) and HepG2.2.15 cells (HBV-expressing stable cell line), which is a kind gift of Dr. Tatsuo Kanda, Japan, were maintained in RPMI 1640 medium (HyClone, GE Healthcare). All cell lines were supplemented with 10% fetal bovine serum (Gibco, Invitrogen) and penicillin/streptomycin (Gibco, Invitrogen) at 37 °C in 5% (v/v) CO_2. Transfection was done with Lipofectamine 2000 (Invitrogen) as per the manufacturer's protocol, whereas INTERFERin transfection reagent (Polyplus) was used according to the manufacturer's protocol for transfecting with Sp110 siRNA Smart Pool (Santa Cruz Biotechnology; catalog no. sc-76542), Sp110siRNA1(GCACUUCAGUGACCAAUGAdTdT), Sp110siRNA2(GAUCAUUGAUGGCACUUCAdTdT), Sp110siRNA3(GGAUGGAACUUGGUUAACAdTdT), and Sp100siRNA(GUGAGCCUGUGAUCAAUAAdTdT) or negative control siRNA pool (Invitrogen). TSA treatment was done at 300 ng/ml for 16 h.

Plasmids

Human cDNA clone of *SP110*, transcript variant c, was purchased from Origene (catalog no. SC124278). Sp110c (full length), Sp110-SPB (C terminus of Sp110 spanning from residues 443–713, harboring the chromatin-binding modules SAND, PHD, and bromodomain), and Sp110 N-terminus (Sp100-domain-containing module; residues from 1 to 450) were subcloned into pdcDNA-FLAG vector using GATEWAY cloning strategy. Plasmids FLAG-SENP1 (catalog no. 17357), FLAG-SENP2 (catalog no. 18047), pGFP-HBX (catalog no. 24931), and HBx-HA (catalog no. 24930) were procured from

Addgene. The 1.3-mer HBV plasmid and 1.3-mer HBV X-null plasmid as used in previous studies (59, 60) were obtained as kind gifts. Construct for luciferase assay was done by cloning the promoter region of the *STAT1* gene harboring an ISRE site (61) along with the Sp110-binding site in the luciferase expression vector pGL3-Basic.

Co-immunofluorescence and confocal microscopy

The cells were fixed with 4% paraformaldehyde (Sigma) in PBS at room temperature and permeabilized with 1% Triton X-100 in PBS followed by blocking with 3% BSA in PBS. Cells were then incubated for 1 h at room temperature with primary antibody and washed three times with PBST (PBS + 0.05% Tween 20). The coverslips were then incubated with Alexa-conjugated secondary antibody (Alexa 488 and 594, Invitrogen) for 1 h in the dark at room temperature, washed with PBST, and mounted with mounting media. The antibodies used are listed in supplemental Table S2. Finally, the imaging was done with Nikon Ti-E confocal microscope with A1RMP scanner head and Zeiss LSM 510 meta confocal microscope. All images within each sample set were captured using identical confocal settings. The co-localization measurements between the immunolabels were estimated by the Pearson's coefficient, which was obtained by analyzing the images with NIS-Elements AR Analysis 3.13.00.

Immunohistochemistry staining

IHC staining was executed with liver tissues. The slides were first heated at 70 °C for 30 min followed by a 5-min wash in xylene, 100, 95, and 80% ethanol, and pure distilled water. Heat-induced antigen retrieval was done in 10 mM sodium citrate (pH 6.0) followed by blocking in universal blocking solution (Thermo Fisher Scientific). The slides were then incubated with anti-Sp110 (Sigma) antibody for 1 h, washed with TBST, and incubated with HRP-tagged secondary antibody. The stain was developed with 3,3′-diaminobenzidine (Sigma) and counter-stained with hematoxylin. The sections were then mounted with coverslips with DPX (Thermo Fisher Scientific) for microscopic imaging. The quantification of the positively stained area was done with ImageJ software.

Cell lysis and immunoblotting

For Western blotting, cells were harvested and lysed with Laemmli buffer (120 mM Tris-HCl (pH 6.8), 20% glycerol, and 4% SDS). The lysates with equal amounts of protein were then run in SDS-PAGE and transferred to nitrocellulose membrane (Millipore, HATF00010). Following incubation with primary antibody (overnight at 4 °C) and HRP-conjugated secondary antibody (3 h at room temperature), the blots were developed using a chemiluminescent substrate (Millipore, WBKLS0500). Densitometry measurements of bands were used for quantification of each marker by integrating each peak in ImageJ software.

Quantitative real-time PCR (qRT-PCR)

Total RNA was extracted using TRIzol (Himedia). Complementary DNA was synthesized from 2.5 μg of total RNA using Revertaid fast strand cDNA synthesis kit (Thermo Fisher Scientific) according to the manufacturer's protocol followed by qRT-PCR using 2× power SYBR Green mix (Applied Biosystems). qRT-PCR was performed using 7500 real-time PCR machine (Applied Biosystems). The primers used are listed in supplemental Table S1. The amount of target mRNA in the sample was calculated by normalizing with respect to the housekeeping genes (18s rRNA or GAPDH). Fold-change of the gene in the experiment was calculated by $2^{-\Delta\Delta}C_T$, where $\Delta C_T (C_{T\text{-target gene}} - C_{T\text{-GAPDH}})$ and $\Delta\Delta C_T = \Delta C_{T\,(\text{Experiment})} - \Delta C_{T\,(\text{Control})}$.

Co-immunoprecipitation (co-IP)

The cells were cross-linked with 1% formaldehyde at room temperature for 10 min, and the reaction was stopped by adding 0.125 M glycine and incubated for 10 min, and then co-IP was performed as described previously (62). Concisely, after cross-linking, the cells were lysed with 50 mM HEPES (pH 7.5), 150 mM NaCl, 1.5 mM $MgCl_2$, 1 mM EDTA, 1 mM EGTA, 1% Triton X-100, 0.5% sodium deoxycholate, 5% glycerol, 1 mM DTT, 2 mM PMSF, 10 mM *N*-ethylmaleimide complete protease inhibitor mixture and incubated on ice for 1 h followed by sonication and centrifugation at 16,000 × *g* for 10 min at 4 °C. The lysates, after pre-clearing, were incubated with corresponding antibodies overnight, followed by a 2-h incubation with pre-blocked Dynabeads (Invitrogen). The beads were then washed three times with lysis buffer and boiled with SDS dye, and the eluted complex was subjected to immunoblotting.

Chromatin immunoprecipitation (ChIP)

ChIP assays were performed as described previously (62). Briefly, cells were cross-linked with 1% formaldehyde at room temperature for 10 min, and the reaction was stopped by adding 0.125 M glycine and incubated for 10 min. Cells were lysed in cell lysis buffer (5 mM PIPES (pH 8.0), 85 mM KCl, 0.5% Nonidet P-40, 1× protease inhibitor cocktail), the isolated nuclei were then resuspended in nuclei lysis buffer (50 mM Tris-HCl (pH 8.0), 10 mM EDTA, 1% SDS, 1× protease inhibitor cocktail). After sonication and pre-clearing, the chromatin was immunoprecipitated with anti-HBX (Abcam), anti-p300 (Abcam), and anti-HDAC1 (Abcam) antibodies overnight at 4 °C. DYNA-beads blocked overnight with 0.3 mg/ml salmon sperm DNA were added to the lysate and incubated for 2 h. Beads were washed with RIPA buffer (50 mM Tris-HCl, pH 8.0, 150 mM NaCl, 0.1% SDS, 0.5% sodium deoxycholate, 1% Nonidet P-40, 1 mM EDTA), high-salt buffer (50 mM Tris-HCl, pH 8.0, 500 mM NaCl, 0.1% SDS, 0.5% sodium deoxycholate, 1% Nonidet P-40, 1 mM EDTA), LiCl buffer (50 mM Tris-HCl, pH 8.0, 250 mM LiCl, 0.5% sodium deoxycholate, 1% Nonidet P-40, 1 mM EDTA), and Tris-EDTA buffer (10 mM Tris-HCl, pH 8.0, 1 mM EDTA), consecutively. Following RNase A and proteinase K treatment, the beads were kept for de-cross-linking at 65 °C. Phenol/chloroform extraction followed ethanol precipitation was performed. The DNA pellet was dissolved in H_2O and placed for qPCR analysis using gene-specific primers. ChIP with non-specific antibody (IgG) was done to normalize the enrichment of the specific factor on the target site.

Analysis of HBV viral properties

0.4×10^6 cells were seeded in each well of a 6-well dish for the experiments. After the transfection and/or treatments were done, total DNA was extracted from 200 μl of culture supernatant using Qiagen blood mini-kit (catalog no. 51104). HBV viral load was subsequently quantified by real-time assay using NIBSC standards as described earlier (63, 64). HBsAg levels were analyzed by using commercial ELISA kits (Diasorin, catalog no. ETI-AB-AUK-3).

Additionally, the DNA samples were subjected to nested PCR as in previous studies (65) to amplify the hepatitis B surface antigen region using primers HBV1 and HBV2 (for first-round PCR) and HBV3 and HBV4 (for second-round PCR). An equal volume of DNA extract was added to the reaction mixture containing a final concentration of 10 mM Tris-HCl (pH 8.3), 50 mM KCl, 1.5 mM $MgCl_2$, 0.2 mM of each dNTPs, 2.5 units of *Taq* polymerase (Promega, GoTaq), and 0.6 mM of each primer. The cycle conditions were as follows: denaturation at 94 °C for 2 min and 30 s, followed by 35 cycles at 94 °C for 1 min, 56 °C for 1 min, and 72 °C for 2 min, with a 10-min extension step at 72 °C at the end. For second-round PCR, the annealing temperature was increased to 60 °C and the final PCR products were subjected to gel electrophoresis to analyze the extent of HBV infection.

Study subjects

Clinical samples were obtained with patient consent from Indian Council of Medical Research (ICMR) virus unit, ID&BG Hospital Campus, Kolkata, India. The samples were mainly sub-grouped into the following categories: normal (patients without having any HBV, HCV, or HIV background) and patients with high HBV DNA load in serum ($>10^5$ copies/ml). The sp110 level was detected for $n = 15$ samples in each category. CHB samples were obtained from Kalinga Gastroenterology Foundation (Cuttack, India). Samples from patients with steatosis but no history of HCV, HBV, or HIV were also considered as disease control. The informed patient consent form was approved by the institutional ethics committee. The AASLD 2009 guidelines were followed for the diagnosis of patients with CHB. Additionally, we procured commercial tissue microarray (Abcam, catalog no. ab178209), and a total of 10 hepatitis samples were analyzed by IHC.

Southern blotting

DNA was isolated from HBV-infected cells by modified Hirt extraction and subjected to Southern blotting as described previously (22). Briefly, extracted DNA was electrophoresed in 1.2% agarose gel in 1× TAE buffer at low voltage for 5 h. The gel was then soaked in Depurination buffer (0.2 M HCl) for 10 min, followed by 1-h incubation with slow shaking, first in denaturing buffer (0.5 M NaOH, 1.5 M NaCl) and then in neutralizing buffer (1.5 M NaCl, 1 M Tris-HCl (pH 7.4)). Finally, the gel was submerged in 20× SSC (3 M NaCl, 0.3 M sodium citrate) for 30 min. The DNA was transferred to an Immobilon-NY^+ membrane (Millipore, INYC00010) through capillary transfer for 72 h. The membrane was then cross-linked by exposure to UV light (254 nM) in a CL-1000 Ultraviolet Stratalinker (UVP) for a total dose of 120 mJ/cm^2. HBV DNA was then detected by incubating with end-labeled probes as used in previous studies (49).

ELISA

Standard indirect ELISA protocol was followed. Briefly, serum samples were incubated in the plates at 4 °C overnight. The plate was then washed, incubated with blocking buffer (3% BSA in PBST) for 1 h, washed, incubated with the anti-Sp110 antibody (1:200), and washed followed by incubation with secondary antibody. The plate was then thoroughly washed, and TMB reagent was added as substrate and incubated for 15 min, and absorbance was taken at 450 nm.

Luciferase assay

For reporter assay, cells were seeded in 12-well culture plates. After 24 h, pGL3-*STAT1* promoter construct or pGL3-basic vector was co-transfected with FLAG-Sp110 or FLAG-Empty vector with Lipofectamine 2000 (Invitrogen). Each transfection was normalized with the pRL-CMV vector. The cells were harvested the next day with passive lysis buffer and firefly/*Renilla* luciferase activity was determined using the manufacturer's protocol (Dual-Luciferase Reporter Assay System, Promega, catalog no. E1910) Each transfection was performed in triplicate, and the experiments were repeated three times.

Flow cytometry

For cell cycle analysis, cells were harvested, thoroughly resuspended in PBS, and then fixed by adding an equal volume of chilled 100% ethanol (Merck), dropwise, with continuous vortexing. After overnight incubation at −20 °C, the mixture was centrifuged, and the cells were freshly resuspended in PBS. Cells were then incubated with RNase A for 30 min followed 1 h with propidium iodide (Sigma). Flow cytometric data acquisition was performed on BD FACSCalibur platform.

Apoptosis assay

Apoptosis assay was done using ENZO ApoStrand ELISA apoptosis detection kit (BML-AK120) according to the manufacturer's protocol. Briefly, cells were treated with Fixative (BML-KI172) for 30 min and dried by keeping the plate at 56 °C for 20 min. Cells were treated with 100% formamide (BML-KI165), kept at room temperature for 10 min, and followed by heat at 56 °C to denature DNA in apoptotic cells. The cells were then incubated with Blocking Solution (BML-KI168) for 1 h at 37 °C and then with Antibody Mixture (BML-KI166) at room temperature for 30 min. The plate was rinsed three times with Wash Buffer (BML-KI170). Peroxidase substrate (BML-KI169) was added to each well and incubated for 30 min; absorbance at 405 nm was recorded.

Microarray analysis

Raw data from three independent biological experiments were normalized using robust multi-array average (RMA), and baseline transformation was done to the median of the samples by GeneSpring GX 12.5 software (Agilent Technologies Inc, Santa Clara, CA). Differentially expressed probe sets upon Sp110 silencing in HepG2.2.15 cells compared with negative control silenced cells were noted by applying the Volcano Plot

using a fold-change threshold of absolute fold-change greater than or equal to 1.5 (or mentioned otherwise) and a statistically significant *t* test *p* value threshold adjusted for false discovery rate of less than 0.001. Analytically significant genes with *p* value adjusted for a false discovery rate of less than 0.05 derived using the hypergeometric distribution test corresponding to differentially expressed genes were decided using a paired *t* test. STRING network analysis has been used to find the clusters among the differentially expressed genes (absolute fold-change of >2, minimum required interaction score: high confidence, 0.7). The complete gene list (supplemental Table S3) and the enriched processes list (supplemental Table S4; list of most affected pathways) upon Sp110 silencing obtained from microarray have been appended in the supplemental material.

The direct targets of HBx, which are co-regulated by Sp110, were identified by comparing Sp110 silenced microarray data (supplemental Table S3) with the previously reported integrated ChIP-chip and microarray data of HBx (accession number GSE11108) (33) with the following parameters: signal intensity cutoff >1.5, for HBx recruitment on the genes from Chip-on-chip data analysis, and an absolute fold-change of >1.2 for HBx and Sp110 microarray, $p < 0.05$.

Statistical analysis

All the experiments were repeated independently at least three times. Statistical analysis was done using GraphPad unpaired two-tailed Student's *t* test. The statistical significance has been represented as follows: **, $p < 0.01$; *, $p < 0.05$.

Author contributions—C. D. conceived the study and designed the experiments. I. S. designed and performed the experiments and analyzed the data. D. D. performed the experiments. R. C. and S. P. S. contributed reagents/materials that helped in the study design. C. D. and I. S. wrote the paper.

Acknowledgments—We are grateful to Dr. Mashashi Mizokami (Japan) and Dr. Wang-Shick Ryu (South Korea) for their kind gifts of 1.3-mer HBV and 1.3-mer HBV X-null plasmids. The Southern blot experiments were done in the laboratory of Dr. Suvendra Nath Bhattacharyya of CSIR-Indian Institute of Chemical Biology, who kindly allowed us to use his facility to perform the Southern blot experiments. We also acknowledge the technical help of Mainak Bose from the same laboratory in this regard. We are grateful to Dr. Oishee Chakrabarti for kind assistance with the Zeiss confocal microscope. We thank Payal Chakraborty and Madavan Vasudevan from Bionivid Technology, Pvt. Ltd., for their assistance with microarray experiments and data analysis. We acknowledge Dr. Siddhartha Roy, Indian Institute of Chemical Biology, for critical comments on the manuscript and helping out on initial study design. We also acknowledge Santanu Adhikary and Santanu Ghosh for their contribution in this study.

References

1. Mhamdi, M., Funk, A., Hohenberg, H., Will, H., and Sirma, H. (2007) Assembly and budding of a hepatitis B virus is mediated by a novel type of intracellular vesicles. *Hepatology* **46,** 95–106
2. Gearhart, T. L., and Bouchard, M. J. (2010) Replication of the hepatitis B virus requires a calcium-dependent HBx-induced G_1 phase arrest of hepatocytes. *Virology* **407,** 14–25
3. Hu, L., Chen, L., Li, L., Sun, H., Yang, G., Chang, Y., Tu, Q., Wu, M., and Wang, H. (2011) Hepatitis B virus X protein enhances cisplatin-induced hepatotoxicity via a mechanism involving degradation of Mcl-1. *J. Virol.* **85,** 3214–3228
4. Zhang, T., Xie, N., He, W., Liu, R., Lei, Y., Chen, Y., Tang, H., Liu, B., Huang, C., and Wei, Y. (2013) An integrated proteomics and bioinformatics analyses of hepatitis B virus X interacting proteins and identification of a novel interactor apoA-I. J. *Proteomics* **84,** 92–105
5. Möller, A., and Schmitz, M. L. (2003) Viruses as hijackers of PML nuclear bodies. *Arch. Immunol. Ther. Exp.* **51,** 295–300
6. Zhang, X., Hou, J., and Lu, M. (2013) Regulation of hepatitis B virus replication by epigenetic mechanisms and microRNAs. *Front. Genet.* **4,** 202
7. Decorsière, A., Mueller, H., van Breugel, P. C., Abdul, F., Gerossier, L., Beran, R. K., Livingston, C. M., Niu, C., Fletcher, S. P., Hantz, O., and Strubin, M. (2016) Hepatitis B virus X protein identifies the Smc5/6 complex as a host restriction factor. *Nature* **531,** 386–389
8. Bloch, D. B., Nakajima, A., Gulick, T., Chiche, J. D., Orth, D., de La Monte, S. M., and Bloch, K. D. (2000) Sp110 localizes to the PML-Sp100 nuclear body and may function as a nuclear hormone receptor transcriptional coactivator. *Mol. Cell. Biol.* **20,** 6138–6146
9. Nicewonger, J., Suck, G., Bloch, D., and Swaminathan, S. (2004) Epstein-Barr virus (EBV) SM protein induces and recruits cellular Sp110b to stabilize mRNAs and enhance EBV lytic gene expression. *J. Virol.* **78,** 9412–9422
10. Watashi, K., Hijikata, M., Tagawa, A., Doi, T., Marusawa, H., and Shimotohno, K. (2003) Modulation of retinoid signaling by a cytoplasmic viral protein via sequestration of Sp110b, a potent transcriptional corepressor of retinoic acid receptor, from the nucleus. *Mol. Cell. Biol.* **23,** 7498–7509
11. Wang, T., Ong, P., Roscioli, T., Cliffe, S. T., and Church, J. A. (2012) Hepatic veno-occlusive disease with immunodeficiency (VODI): First reported case in the U.S., and identification of a unique mutation in Sp110. *Clin. Immunol.* **145,** 102–107
12. Png, E., Alisjahbana, B., Sahiratmadja, E., Marzuki, S., Nelwan, R., Adnan, I., van de Vosse, E., Hibberd, M., van Crevel, R., Ottenhoff, T. H., and Seielstad, M. (2012) Polymorphisms in SP110 are not associated with pulmonary tuberculosis in Indonesians. *Infect. Genet. Evol.* **12,** 1319–1323
13. Liang, L., Zhao, Y. L., Yue, J., Liu, J. F., Han, M., Wang, H., and Xiao, H. (2011) Association of SP110 gene polymorphisms with susceptibility to tuberculosis in a Chinese population. *Infect. Genet. Evol.* **11,** 934–939
14. Cai, L., Deng, S.-L., Liang, L., Pan, H., Zhou, J., Wang, M.-Y., Yue, J., Wan, C.-L., He, G., and He, L. (2013) Identification of genetic associations of SP110/MYBBP1A/RELA with pulmonary tuberculosis in the Chinese Han population. *Hum. Genet.* **132,** 265–273
15. Thye, T., Browne, E. N., Chinbuah, M. A., Gyapong, J., Osei, I., Owusu-Dabo, E., Niemann, S., Rüsch-Gerdes, S., Horstmann, R. D., and Meyer, C. G. (2006) No associations of human pulmonary tuberculosis with Sp110 variants. *J. Med. Genet.* **43,** e32
16. Wu, Y., Guo, Z., Yao, K., Miao, Y., Liang, S., Liu, F., Wang, Y., and Zhang, Y. (2016) The transcriptional foundations of Sp110-mediated macrophage (RAW264.7) resistance to mycobacterium tuberculosis H37Ra. *Sci. Rep.* **6,** 22041
17. Cai, L., Wang, Y., Wang, J.-F., and Chou, K.-C. (2011) Identification of proteins interacting with human SP110 during the process of viral infections. *Med. Chem.* **7,** 121–126
18. Shamay, M., Barak, O., Doitsh, G., Ben-Dor, I., and Shaul, Y. (2002) Hepatitis B virus pX interacts with HBXAP, a PHD finger protein to coactivate transcription. *J. Biol. Chem.* **277,** 9982–9988
19. Sells, M. A., Zelent, A. Z., Shvartsman, M., and Acs, G. (1988) Replicative intermediates of hepatitis B virus in HepG2 cells that produce infectious virions. *J. Virol.* **62,** 2836–2844
20. Cheng, Z., Zhi, X., Sun, G., Guo, W., Huang, Y., Sun, W., Tian, X., Zhao, F., and Hu, K. (2016) Sodium selenite suppresses hepatitis B virus transcription and replication in human hepatoma cell lines. *J. Med. Virol.* **88,** 653–663
21. Cheng, Z., Sun, G., Guo, W., Huang, Y., Sun, W., Zhao, F., and Hu, K. (2015) Inhibition of hepatitis B virus replication by quercetin in human hepatoma cell lines. *Virol. Sin.* **30,** 261–268
22. Cai, D., Nie, H., Yan, R., Guo, J.-T., Block, T. M., and Guo, H. (2013) A Southern blot assay for detection of hepatitis B virus covalently closed circular DNA from cell cultures. *Methods Mol. Biol.* **1030,** 151–161

23. Niu, C., Livingston, C. M., Li, L., Beran, R. K., Daffis, S., Ramakrishnan, D., Burdette, D., Peiser, L., Salas, E., Ramos, H., Yu, M., Cheng, G., Strubin, M., Delaney, W. E., IV, and Fletcher, S. P. (2017) The Smc5/6 complex restricts HBV when localized to ND10 without inducing an innate immune response and is counteracted by the HBV X protein shortly after infection. *PLoS ONE* **12,** e0169648
24. Sternsdorf, T., Jensen, K., Reich, B., and Will, H. (1999) The nuclear dot protein Sp100, characterization of domains necessary for dimerization, subcellular localization, and modification by small ubiquitin-like modifiers. *J. Biol. Chem.* **274,** 12555–12566
25. Kumar, A., and Zhang, K. Y. (2015) Advances in the development of SUMO specific protease (SENP) inhibitors. *Comput. Struct. Biotechnol. J.* **13,** 204–211
26. Liu, H., Yuan, Y., Guo, H., Mitchelson, K., Zhang, K., Xie, L., Qin, W., Lu, Y., Wang, J., Guo, Y., Zhou, Y., and He, F. (2012) Hepatitis B virus encoded X protein suppresses apoptosis by inhibition of the caspase-independent pathway. *J. Proteome Res.* **11,** 4803–4813
27. Arzberger, S., Hösel, M., and Protzer, U. (2010) Apoptosis of hepatitis B virus-infected hepatocytes prevents release of infectious virus. *J. Virol.* **84,** 11994–12001
28. Szklarczyk, D., Franceschini, A., Wyder, S., Forslund, K., Heller, D., Huerta-Cepas, J., Simonovic, M., Roth, A., Santos, A., Tsafou, K. P., Kuhn, M., Bork, P., Jensen, L. J., and von Mering, C. (2015) STRING v10: protein-protein interaction networks, integrated over the tree of life. *Nucleic Acids Res.* **43,** D447–D452
29. Génin, P., Morin, P., and Civas, A. (2003) Impairment of interferon-induced IRF-7 gene expression due to inhibition of ISGF3 formation by trichostatin A. *J. Virol.* **77,** 7113–7119
30. Chang, H.-M., Paulson, M., Holko, M., Rice, C. M., Williams, B. R., Marié, I., and Levy, D. E. (2004) Induction of interferon-stimulated gene expression and antiviral responses require protein deacetylase activity. *Proc. Natl. Acad. Sci. U.S.A.* **101,** 9578–9583
31. Kew, M. C. (2011) Hepatitis B virus x protein in the pathogenesis of hepatitis B virus-induced hepatocellular carcinoma. *J. Gastroenterol. Hepatol.* **26,** 144–152
32. Cromlish, J. A. (1996) Hepatitis B virus-induced hepatocellular carcinoma: possible roles for HBx. *Trends Microbiol.* **4,** 270–274
33. Sung, W. K., Lu, Y., Lee, C. W., Zhang, D., Ronaghi, M., and Lee, C. G. (2009) Deregulated direct targets of the hepatitis B virus (HBV) protein, HBx, identified through chromatin immunoprecipitation and expression microarray profiling. *J. Biol. Chem.* **284,** 21941–21954
34. Cougot, D., Wu, Y., Cairo, S., Caramel, J., Renard, C. A., Lévy, L., Buendia, M. A., and Neuveut, C. (2007) The hepatitis B virus X protein functionally interacts with CREB-binding protein/p300 in the regulation of CREB-mediated transcription. *J. Biol. Chem.* **282,** 4277–4287
35. Shon, J. K., Shon, B. H., Park, I. Y., Lee, S. U., Fa, L., Chang, K. Y., Shin, J. H., and Lee, Y. I. (2009) Hepatitis B virus-X protein recruits histone deacetylase 1 to repress insulin-like growth factor binding protein 3 transcription. *Virus Res.* **139,** 14–21
36. Choi, J., Chang, J. S., Song, M. S., Ahn, B. Y., Park, Y., Lim, D. S., and Han, Y. S. (2003) Association of hepatitis B virus polymerase with promyelocytic leukemia nuclear bodies mediated by the S100 family protein p11. *Biochem. Biophys. Res. Commun.* **305,** 1049–1056
37. Wang, W. H., Studach, L. L., and Andrisani, O. M. (2011) Proteins ZNF198 and SUZ12 are down-regulated in hepatitis B virus (HBV) X protein-mediated hepatocyte transformation and in HBV replication. *Hepatology* **53,** 1137–1147
38. Chung, Y. L., and Wu, M. L. (2013) Promyelocytic leukaemia protein links DNA damage response and repair to hepatitis B virus-related hepatocarcinogenesis. *J. Pathol.* **230,** 377–387
39. Duprez, E., Saurin, A. J., Desterro, J. M., Lallemand-Breitenbach, V., Howe, K., Boddy, M. N., Solomon, E., de Thé, H., Hay, R. T., and Freemont, P. S. (1999) SUMO-1 modification of the acute promyelocytic leukaemia protein PML: implications for nuclear localisation. *J. Cell Sci.* **112,** 381–393
40. Ohbayashi, N., Kawakami, S., Muromoto, R., Togi, S., Ikeda, O., Kamitani, S., Sekine, Y., Honjoh, T., and Matsuda, T. (2008) The IL-6 family of cytokines modulates STAT3 activation by desumoylation of PML through SENP1 induction. *Biochem. Biophys. Res. Commun.* **371,** 823–828
41. Kim, Y. H., Sung, K. S., Lee, S. J., Kim, Y. O., Choi, C. Y., and Kim, Y. (2005) Desumoylation of homeodomain-interacting protein kinase 2 (HIPK2) through the cytoplasmic-nuclear shuttling of the SUMO-specific protease SENP1. *FEBS Lett.* **579,** 6272–6278
42. Meinecke, I., Cinski, A., Baier, A., Peters, M. A., Dankbar, B., Wille, A., Drynda, A., Mendoza, H., Gay, R. E., Hay, R. T., Ink, B., Gay, S., and Pap, T. (2007) Modification of nuclear PML protein by SUMO-1 regulates Fas-induced apoptosis in rheumatoid arthritis synovial fibroblasts. *Proc. Natl. Acad. Sci. U.S.A.* **104,** 5073–5078
43. Wang, Q., Xu, Y., Zhou, W., Zhong, L., Wen, Z., Yu, H., Chen, S., Shen, J., Chen, H., She, Q., Jiang, J., Miao, J., and Wei, W. (2014) The viral oncoprotein HBx of hepatitis b virus promotes the growth of hepatocellular carcinoma through cooperating with the cellular oncoprotein RMP. *Int. J. Biol. Sci.* **10,** 1181–1192
44. Chae, S., Ji, J. H., Kwon, S. H., Lee, H. S., Lim, J. M., Kang, D., Lee, C. W., and Cho, H. (2013) HBxAPα/Rsf-1-mediated HBx-hBubR1 interactions regulate the mitotic spindle checkpoint and chromosome instability. *Carcinogenesis* **34,** 1680–1688
45. Truant, R., Antunovic, J., Greenblatt, J., Prives, C., and Cromlish, J. (1995) A direct interaction of the hepatitis B virus HBx protein with p53 leads to inhibition by HBx of p53 response element-directed transactivation. *J. Virol.* **69,** 1851–1859
46. Wang, H., and Ryu, W. S. (2010) Hepatitis B virus polymerase blocks pattern recognition receptor signaling via interaction with DDX3: implications for immune evasion. *PLoS Pathog.* **6,** e1000986
47. Wu, J., Meng, Z., Jiang, M., Pei, R., Trippler, M., Broering, R., Bucchi, A., Sowa, J. P., Dittmer, U., Yang, D., Roggendorf, M., Gerken, G., Lu, M., and Schlaak, J. F. (2009) Hepatitis B virus suppresses toll-like receptor-mediated innate immune responses in murine parenchymal and nonparenchymal liver cells. *Hepatology* **49,** 1132–1140
48. Chen, J., Wu, M., Zhang, X., Zhang, W., Zhang, Z., Chen, L., He, J., Zheng, Y., Chen, C., Wang, F., Hu, Y., Zhou, X., Wang, C., Xu, Y., Lu, M., and Yuan, Z. (2013) Hepatitis B virus polymerase impairs interferon-α-induced STA T activation through inhibition of importin-α5 and protein kinase C-δ. *Hepatology* **57,** 470–482
49. Köck, J., Rösler, C., Zhang, J., Blum, H. E., Nassal, M., and Thoma, C. (2012) Human hepatitis B virus production in avian cells is characterized by enhanced RNA splicing and the presence of capsids containing shortened genomes. *PLoS ONE* 7, e37248
50. Cheon, H., Holvey-Bates, E. G., Schoggins, J. W., Forster, S., Hertzog, P., Imanaka, N., Rice, C. M., Jackson, M. W., Junk, D. J., and Stark, G. R. (2013) IFNβ-dependent increases in STAT1, STAT2, and IRF9 mediate resistance to viruses and DNA damage. *EMBO J.* **32,** 2751–2763
51. Nakao, K., Nakata, K., Yamashita, M., Tamada, Y., Hamasaki, K., Ishikawa, H., Kato, Y., Eguchi, K., and Ishii, N. (1999) p48 is involved in interferon-α-induced suppression of hepatitis B virus enhancer-1 activity. *J. Biol. Chem.* **274,** 28075–28078
52. Silverman, R. H. (2007) Viral encounters with 2′,5′-oligoadenylate synthetase and RNase L during the interferon antiviral response. *J. Virol.* **81,** 12720–12729
53. Gordien, E., Rosmorduc, O., Peltekian, C., Garreau, F., Bréchot, C., and Kremsdorf, D. (2001) Inhibition of hepatitis B virus replication by the interferon-inducible MxA protein. *J. Virol.* **75,** 2684–2691
54. Li, N., Zhang, L., Chen, L., Feng, W., Xu, Y., Chen, F., Liu, X., Chen, Z., and Liu, W. (2012) MxA inhibits hepatitis B virus replication by interaction with hepatitis B core antigen. *Hepatology* **56,** 803–811
55. Guo, J., Hui, D. J., Merrick, W. C., and Sen, G. C. (2000) A new pathway of translational regulation mediated by eukaryotic initiation factor 3. *EMBO J.* **19,** 6891–6899
56. Terenzi, F., Hui, D. J., Merrick, W. C., and Sen, G. C. (2006) Distinct induction patterns and functions of two closely related interferon-inducible human genes, ISG54 and ISG56. *J. Biol. Chem.* **281,** 34064–34071
57. Pichlmair, A., Lassnig, C., Eberle, C. A., Górna, M. W., Baumann, C. L., Burkard, T. R., Bürckstümmer, T., Stefanovic, A., Krieger, S., Bennett, K. L., Rülicke, T., Weber, F., Colinge, J., Müller, M., and Superti-Furga, G.

(2011) IFIT1 is an antiviral protein that recognizes 5′-triphosphate RNA. *Nat. Immunol.* **12,** 624–630

58. Pei, R.-J., Chen, X.-W., and Lu, M.-J. (2014) Control of hepatitis B virus replication by interferons and Toll-like receptor signaling pathways. *World J. Gastroenterol.* **20,** 11618–11629
59. Bandopadhyay, M., Sarkar, N., Datta, S., Das, D., Pal, A., Panigrahi, R., Banerjee, A., Panda, C. K., Das, C., Chakrabarti, S., and Chakravarty, R. (2016) Hepatitis B virus X protein mediated suppression of miRNA-122 expression enhances hepatoblastoma cell proliferation through cyclin G1-p53 axis. *Infect. Agent. Cancer* **11,** 40
60. Hussain, Z., Jung, H. S., Ryu, D. K., and Ryu, W. S. (2009) Genetic dissection of naturally occurring basal core promoter mutations of hepatitis B virus reveals a silent phenotype in the overlapping X gene. *J. Gen. Virol.* **90,** 2272–2281
61. Yuasa, K., and Hijikata, T. (2016) Distal regulatory element of the STAT1 gene potentially mediates positive feedback control of STAT1 expression. *Genes Cells* **21,** 25–40
62. Adhikary, S., Sanyal, S., Basu, M., Sengupta, I., Sen, S., Srivastava, D. K., Roy, S., and Das, C. (2016) Selective recognition of H3.1K36 dimethylation/H4K16 acetylation facilitates the regulation of all-*trans*-retinoic acid (ATRA)-responsive genes by putative chromatin reader ZMYND8. *J. Biol. Chem.* **291,** 2664–2681
63. Mendy, M. E., Kaye, S., van der Sande, M., Rayco-Solon, P., Waight, P. A., Shipton, D., Awi, D., Snell, P., Whittle, H., and McConkey, S. J. (2006) Application of real-time PCR to quantify hepatitis B virus DNA in chronic carriers in The Gambia. *Virol. J.* **3,** 23
64. Olioso, D., Boaretti, M., Ligozzi, M., Lo Cascio, G., and Fontana, R. (2007) Detection and quantification of hepatitis B virus DNA by SYBR green real-time polymerase chain reaction. *Eur. J. Clin. Microbiol. Infect. Dis.* **26,** 43–50
65. Datta, S., Banerjee, A., Chandra, P. K., Chowdhury, A., and Chakravarty, R. (2006) Genotype, phylogenetic analysis, and transmission pattern of occult hepatitis B virus (HBV) infection in families of asymptomatic HBsAg carriers. *J. Med. Virol.* **78,** 53–59